EPJ Web of Conferences **69**, 00012 (2014)
DOI: 10.1051/epjconf/20146900012


# Formation and decay of a hot compound nucleus

B.V. Carlson[1,a], F.T. Dalmolin[1], M. Dutra[1], T.J. Santos[1], S.R. Souza[2,4], and R. Donangelo[3,4]

[1] *Instituto Tecnológico de Aeronáutica, São José dos Campos SP, Brazil*
[2] *Instituto de Física, Universidade Federal de Rio Grande do Sul, Porto Alegre RS, Brazil*
[3] *Instituto de Física, Universidad de la República de Uruguay, Montevideo, Uruguay*
[4] *Instituto de Física, Universidade Federal de Rio de Janeiro, Rio de Janeiro RJ, Brasil*

**Abstract.** The compound nucleus plays an important role in nuclear reactions over a wide range of projectile-target combinations and energies. The limits that angular momentum places on its formation and existence are, for the most part, well understood. The limits on its excitation energy are not as clear. Here we first analyze general geometrical and thermodynamical features of a hot compound nucleus. We then discuss the manners by which it can decay and close by speculating on the high energy limit to its formation and existence.

## 1 Introduction

Niels Bohr introduced the concept of the compound nucleus in order to explain reactions in which an outgoing particle had lost all information of the incoming state (excepting conserved quantities).[1] This could be understood as a process in which the incoming particle is absorbed by the target nucleus to eventually form a long-lived equilibrated system in which all nucleons are bound - the compound nucleus. The system decays when, through their mutual interaction, sufficient energy is given to one of the particles to allow it to escape.

The decay products of the compound nucleus have been experimentally observed over almost the entire range of combinations of projectile and target as well as of energy. Sophisticated models have been developed that describe its low-excitation decay well. However, at extremely high excitation energy, the decay of the compound nucleus yields a large number of fragments whose formation and escape are not yet fully understood. Here we analyze the characteristics that we expect of compound nuclei at such excitation energies from a theoretical viewpoint.

## 2 The properties of hot nuclei

The density of quasi-bound states of a nucleus is the density of states in which all neutrons are in bound single-particle states and all protons are in single particle states that are either bound or in long-lived single particle states well below the Coulomb barrier. These would seem to be the states that one would associate with the long-lived states of Bohr's conception of the compound nucleus. The excitation energy dependence of the density of states was first estimated by Bethe[2] and has

[a] e-mail: brett@ita.br

been the center of a great deal of theoretical and experimental effort [3–5]. All of these calculations of the density of quasi-bound states begin with a static set of single-particle states and analyze their occupation as a function of the temperature. The Helmholtz free energy determined in this manner, $F^*(T)$ is related to the density of states $\omega(E^*)$ by a Laplace transform,

$$e^{-F^*(T)/T} = \int_0^\infty e^{-E^*/T} \omega(E^*)\, dE^*. \tag{1}$$

As a nucleus is heated, however, it expands and becomes less bound. At a sufficiently high temperature, one would expect it to evaporate completely.

### 2.1 Formal discussion

The effects of heating are not taken into account when a static set of single-particle levels are used to calculate the density, but can be estimated from self-consistent calculations. We have considered two approaches to such calculations. In the simplest, we perform temperature-dependent self-consistent mean field calculations restricted to the states that are quasi-bound at the given temperature. Similar calculations were performed long ago by Brack and Quentin (BQ).[6, 7] As the temperature increases, the nucleus expands and decreases in density, as would be expected. However, at higher temperatures, the limitation to quasi-bound states produces truncated occupation probabilities and anomalous tails in the nuclear density.

Another approach, developed by Bonche, Levit and Vautherin, (BLV)[8, 9] takes into account all single-particle states of a heated nucleus in the self-consistency calculation. These include all resonant states as well as the bound ones. However, they also include the continuum states that describe free nucleons rather than those in a nucleus. To obtain the contribution of the bound and resonant states alone, the contribution of the gas of nucleons in continuum states must be subtracted. This is done by performing two self-consistent calculations - one of the nucleus plus gas and another of the gas alone (both with identical Fermi energies) and subtracting the extensive quantities (entropy, excitation energy, baryon density) obtained for the latter from those of the former. Typical results from this type of calculation are shown in Figs. 1a and 1b. The density of the gas is zero at zero temperature and increases with temperature until the nucleus disappears completely, typically at a temperature betwen 9 and 11 MeV.

We have performed calculations using both the BQ and the BLV prescriptions in the self-consistent relativistic Hartree approximation, using both the nonlinear NL3[10] and density-dependent DDME1[11] parameter sets. To our knowledge, these sets provide the best agreement with ground state nuclear masses obtained using the relativistic Hartree approximation. We have also performed calculations using the nonrelativistic BSk14[12] and NRAPR[13] Skyrme interactions in the Thomas-Fermi approximation to the BLV prescription. The BLV results are quite similar in all cases, as can be seen in Figs. 1a and 1b.

### 2.2 Thermodynamic quantities

The extensive quantities that can be obtained from the self-consistent calculations are the entropy, the excitation energy, the baryon and charge density and other density-related quantities, such as deformations and rms radii. The deformation and pairing vanish at extremely low temperatures. Normal isovector pairing usually disappears at temperatures below 1 MeV and almost all calculations yield nuclei that are spherical at 2 MeV.[14] The effects of shell closures are small but still observable at 2 MeV.

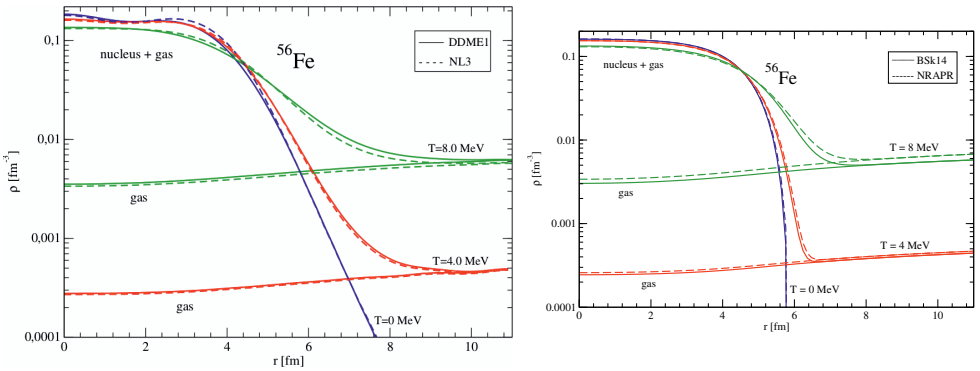


**Figure 1.** (a) Nucleon density using the BLV prescription with the NL3 and DDME1 parametrizations of the relativistic Hartree approximation. (b) Nucleon density using the BLV prescription with the BSk14 and NRAPR Skyrme parametrizations of the Thomas-Fermi approximation.

The entropy and excitation energy are related to the Helmholtz free energy through

$$S^* = -\frac{\partial F^*}{\partial T}, \tag{2}$$

and

$$E^* = F^* - T\frac{\partial F^*}{\partial T} \tag{3}$$

The entropy $S^*(T)$ can be determined directly from the calculations, while the excitation energy is obtained as the difference between the binding energy $E_{bnd}(T)$ at a temperature $T$ and that at temperature zero,

$$E^*(T) = E_{bnd}(T) - E_{bnd}(0) \tag{4}$$

Discounting small effects below a temperature of 1 MeV due to pairing, the entropy in all calculations increases linearly and the excitation quadratically with the temperature up to a temperature of between 4 and 6 MeV. This is the behavior expected of a Fermi gas density of states. Above this temperature, the BQ quantities begin to saturate due to the limited number of single-particle states and fall below the BLV values. The entropy and excitation energy of the BLV calculations maintain the behavior expected of a Fermi gas and remain in good agreement wth each other up to a temperature of about 8 MeV.

Despite the very similar behavior of the entropy and excitation energy of the three sets of calculations below about 6 MeV, we see in the Fig. 2 that their rms radii are very different. The rms radius increases almost linearly in the calculations including only bound single-particle states while it increases quadratically and tends to remain smaller in the cases in which the nucleus is in equilibrium with a surrounding gas. We interpret the smaller radius of the calculations with the BLV prescription as an effect of the pressure exerted by the gas on the hot nucleus. The even smaller radii obtained using the Skyrme interactions could be an artefact of the Thomas-Fermi approximation, in which there are no wave functions and thus no exponentially decaying tails.

We find the rms radii of the relativistic Hartree BLV calculations to be well described by the expression

$$\left\langle r_m^2 \right\rangle = r_{m0}^2 A^{2/3}\left(1 + c_m T^2\right), \tag{5}$$

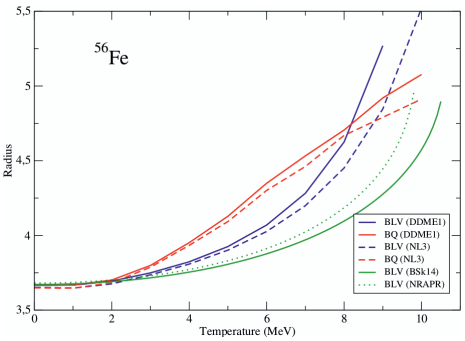


**Figure 2.** Rms radius as a function of the temperature.

where

$$r_{m0} = 0.95 \pm 0.05 \quad \text{f} \qquad \text{and} \qquad c_m = 0.005 \pm 0.001 \quad \text{MeV}^{-2} \,. \tag{6}$$

The nuclear volume is thus about 25% larger at a temperature of 6 MeV than it is in the ground state

## 3 Compound nucleus decay

At low excitation energies, the compound nucleus decays through the sequential emission of light particles from an equilibrated system. Since the system is in equilibrium, the cross section for decay to channel $c$ is given by the product of cross section for formation of the compound nucleus $\sigma_{abs,a}$ times the fraction of the phase space corresponding to the exit channel $c$,

$$\sigma_{ac} = \sigma_{abs,a} \frac{Y_c}{\sum_b Y_b} \,. \tag{7}$$

In the Weisskopf-Ewing approximation,[15, 16] the phase space volume is proportional to the factor $Y_c$,

$$Y_c = (2s_c + 1)\frac{k_c^2}{\pi}\sigma_{abs}(e_c) = (2s_c + 1)\frac{2\mu_c}{\pi\hbar^2} e_c \sigma_{abs}(e_c) \,. \tag{8}$$

At higher excitation energies, this is usually expresed in terms of an integral over a differential factor,

$$Y_c \rightarrow \frac{dY_c}{de_c} = (2s_c + 1)\frac{2\mu_c}{\pi\hbar^2} e_c \sigma_{abs}(e_c)\omega_c(E_c) \,, \tag{9}$$

which is written in terms of the density of final states $\omega_c\,(E_c)$. The Weiskopf-Ewing approximation takes into account energy conservation but does not conserve angular momentum. Both conservation laws are satisfied when the Hauser-Feshbach $Y_c$ factors are used.[17] An alternative formalism, in which classical angular momentum is conserved, was developed by Ericson and Strutinsky[18, 19] and is discussed in the Appendix. In all cases, the cross section for an individual channel can be written in terms of the fraction of the appropriate phase space volume, as in Eq. 7.

A typical example of low energy compound nucleus decay is shown in Fig. 3a, where the cross sections for various emission channels of a neutron-induced reaction on $^{56}$Fe are shown. We see that multiple emission cross sections already dominate above about 15 MeV and grow in complexity as the

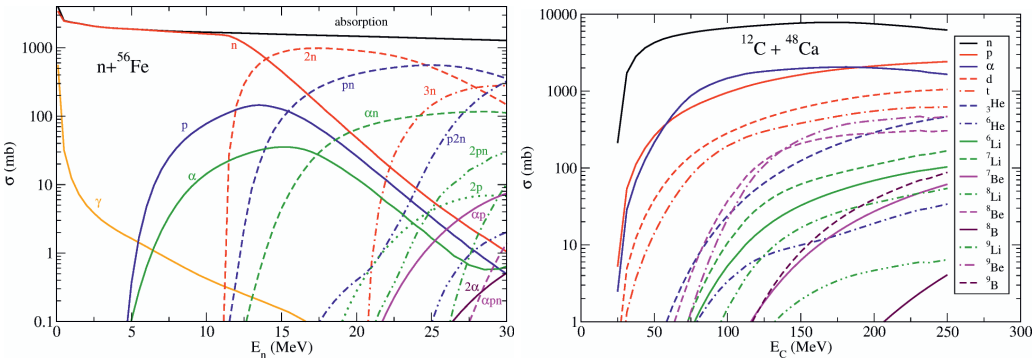


**Figure 3.** (a) Emission cross sections of a neutron-induced reaction on $^{56}$Fe. (b) Production cross sections for the reaction of $^{12}$C + $^{48}$Ca.

incident (and excitation) energy increases. Alternatively, we can look at the production cross sections of the various particles and nuclei emitted from a compound nucleus, as shown for the reaction $^{12}$C + $^{48}$Ca in Fig. 3b. In this case, the reaction cross section is negligible below the carbon energy of about 25 MeV needed to surmount the Coulomb barrier. Only light particles are emitted at energies below a carbon energy of about 60 MeV, corresponding to a temperature of about 3 MeV. As the energy increases above this value, the emission probability of heavier fragments increases until, at sufficiently high energies, several heavy complex fragments can be emitted during the decay. The carbon energy of 250 MeV shown in the figure corresponds to a temperature of about 6 MeV. At such high temperatures, the decay of the compound nucleus is usually modeled as a simultaneous fragmentation into intermediate mass fragments and light particles.

The extent to which intermediate mass fragment emission is simultaneous or sequential has been a subject of theoretical and experimental study for almost 30 years. The statistical multifragmentation model (SMM) [20, 21], an equilibrium model of simultaneous fragment emission, uses the configurations of a statistical ensemble to determine the distribution of primary fragments of a compound nucleus. The primary fragments are then assumed to decay by sequential compound emission or Fermi breakup (FBM) [22]. As the first step toward a more unified model of these processes, we have demonstrated the equivalence of a generalized FBM, in which densities of excited states are taken into account, to the microcanonical version of the SMM.[23]

A drawback of the FBM/SMM model is that it expresses fragment distributions in terms of the probability that are contained in the configurations of a system rather than in terms of their rates of emission. The assumption underlying the model is that every state of every configuration decays at the same rate. To go beyond this, we estimate the decay rate of a configuration as the time rate of change of the density within a given normalization volume. To do so, we use the continuity equation to relate the time rate of change of the probability density to the flux through the surface defining the volume.[24] In this manner, we can establish a link between the unified FBM/SMM and the well-known models of compound nucleus evaporation that permits us to consider simultaneous emission as the limit of an increasingly fast sequential emission process.[25]

An important difference between the usual formulation of compound nucleus evaporation and a general model of sequential emission is that, in the latter, the emission cross sections can no longer be calculated in terms of phase space volumes, as in Eq. 7, which assumes that a very long time elapses between emissions. Instead, they must be calculated dynamically, taking into account the competition

between all modes of decay and the effects of previously emitted particles and fragments that are still close to the decaying compound nucleus. Monte Carlo decay codes, in which each emission is generated randomly according to the competition among the possible decay modes, are appropriate for simulating such a system.

GEMINI++ is one such Monte Carlo decay code.[26–28]. It describes light particle emission using Hauser-Feshbach partial widths and calculates intermediate mass fragment emission and fission partial widths with an effective Weisskopf approximation in which the rotational energy is discounted from the excitation energy. We have modified the code to include a more complete treatment of the effects of angular momentum coupling on intermediate mass fragment emission. We describe the extension including angular momentum coupling in the Appendix.

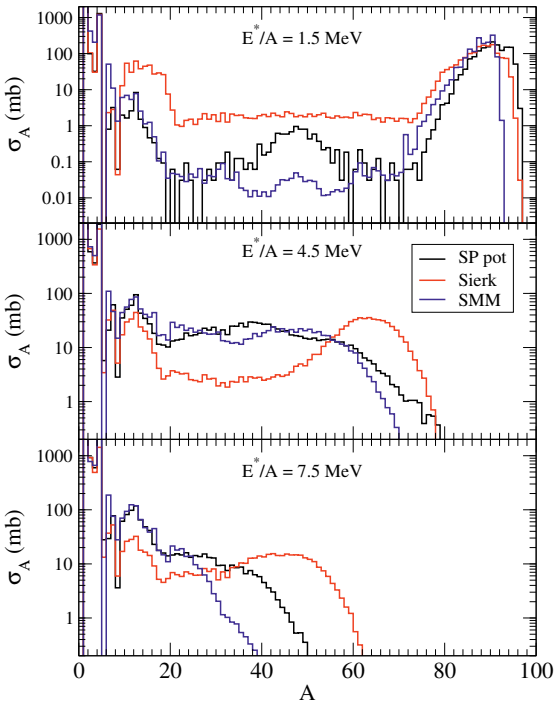


**Figure 4.** Mass distribution of the decay products of an A=100 nucleus at several excitation energies in the standard decay model (Sierk), the enhanced model (SPP) and the statistical multifragmentation model (SMM).

In Figure 4, we compare calculations of the decay of a mass 100 nucleus at three diferent excitation energies using the standard sequential decay model of GEMINI++ , our enhanced sequential decay model and the statistical multifragmentation model. One sees that the enhanced model yields results similar to those of the statistical multifragmentation model. The larger nuclear volume (2 to 3 times the ground state volume) and reduced barriers of the statistical multifragmentation model leaves more energy to excite the fragments and results in smaller fragments and a mass distribution restricted to smaller masses. We would expect a similar shift in the enhanced model, if we were to introduce the large volume expansion of the statistical multifragmentation model. We thus believe that the mass dis-

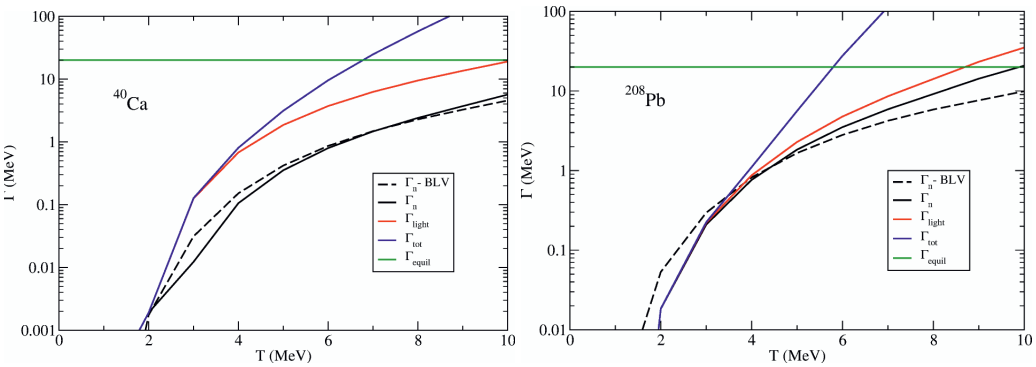


**Figure 5.** (a) Partial widths for the decay of a $^{40}$Ca compound nucleus. The curves are explained in detail in the text. (b) Partial widths for the decay of a $^{208}$Pb compound nucleus.

tribution originating from the simultaneous fragmentation of the statistical multifragmentation model can indeed be described within a sequential emission model.

## 4 Formation of the compound nucleus

Formation of the compound nucleus is limited by both energy and angular momentum. At low energy, barrier transmission determines the formation rate. At higher energies, the angular momentum barrier begins to limit fusion. Light nuclear systems that reach a small enough separation to interact strongly invariably fuse to form a compound nucleus. As the energy increases, the angular momentum barrier prohibits this approximation and thus limits formation of the compound nucleus. In sufficiently heavy systems, a dinuclear system equilibrated in charge and energy could be considered the first stage of the compound nucleus. Depending on the asymmetry of the system, the dinucleus could either evolve rapidly to a spherical compound nucleus or more slowly to a symmetrical dinuclear system, during which it could decay in the process known as quasi-fission. Given the microscopic equilibrium of such a system, we might consider it to be a (highly deformed) compound nucleus as well.

However, our principal point of interest here is to determine the limit in excitation energy to the formation of the compound nucleus. One way to approach this problem is to argue that a compound nucleus cannot form if it decays before it is formed. Since we expect the compound nucleus to be an equilbrated system, we can take the time for equilibration in energy as a lower limit to the formation time. The equilbration time, on the other hand, can be estimated in terms of the width of a typical nuclear state. This width has been investigated in great detail and has a value of about 20 MeV in s-d shell nuclei.[29] This corresponds to a time of about 10 fm/c, roughly the time it would take light to travel from one side of the nucleus to the other.

We thus propose to compare the equilibration width $\Gamma_{equil} = 20$ MeV with the partial widths obtained from the decay model to obtain a limit on the formation of the compound nucleus. In passing, we note that the BLV formalism also provides us with an estimate of the neutron and proton partial widths in terms of the flux of gas incident on the nucleus. In Fig. 5, we see that the BLV neutron partial width is in quite good agreement with the partial neutron decay width in the Weisskopf approximation, giving weight to the interpretation of the model as a compound nucleus in equilibrium with its decay products. In the figure, we also include the contribution of light charged particles to the decay width ($\Gamma_{light}$), as well as the contribution of intermediate fragment emission, to obtain the total width (($\Gamma_{tot}$).

We see that intermediate mass fragment emission becomes important at temperatures of about 4 MeV in both light and heavy nuclei and dominates the total width at higher energies. At a temperature of 5 MeV, intermediate mass fragment emission constitutes about 50% of the decay width of $^{40}$Ca and about 80% of the decay width of $^{208}$Pb. Using the equilibrium width as a criterion for formation of the compound nucleus, we conclude that a light compound nucleus such as $^{40}$Ca cannot form at temperatures above about 6.5 MeV while a heavy system like $^{208}$Pb cannot form a compound nucleus at temperatures above about 5.5 MeV.

## 5 Conclusions

We have briefly reviewed the basic properties of hot compound nuclei, their modes of decay and limits to their formation. We have seen that, between temperatures $T$ of about 1 MeV and 8 to 9 MeV, a hot nucleus has statistical properties that are well approximated by those of a Fermi gas, but a volume that increases with $T^2$ to about 5/4 the ground state volume at $T = 6$ MeV.

In our discussion of decay of the compound nucleus, we noted that light particle emission is the principal decay mode at low excitation energies (excluding the fission of very heavy nuclei) but that intermediate mass fragment emission grows quickly in importance above temperatures of about 4 MeV and becomes the dominant decay mode above about 5 MeV. We have also seen that the sequential emission model and the simultaneous multifragmentation model can be placed on a common footing and furnish similar residual mass distributions. Experimental spallation cross sections have also been found to be well described by a fast but sequential emission process.[30] One can show that a dynamical sequential decay model can also produce the fragment-fragment correlations expected from simultaneous multifragmentation. [31] Here, at least, the decay of a hot equilibrated compound nucleus could be considered to take place through a fast sequential emission process. This is just the natural limit of the slower decay process that occurs at lower excitation energies.

Taking the typical energy spreading width of states in s-d shell nuclei as a measure of the time for equilibration in energy, we have proposed that it can also serve as a limit to the formation of a compound nucleus, by comparison with the corresponding decay time. We conclude from this comparison that an equilibrated compound nucleus cannot be formed at temperatures above about 6 MeV, as it will decay before its formation is complete. Interestingly, this limiting temperature is in agreement with the typical limiting temperature found in experimental caloric curves, where it is interpreted as an indication of a phase transition in nuclear matter.[32] It is also often used as a justification for a multifragmentation description of the decay of the compound nucleus. Here, one might indeed be able to interpret the decay as multifragmentation, but as a nonequlibrium process rather than the result of an equilibrium phase transition. Much work is needed, however, to better understand the transition from equilibrium to nonequilibrium that is expected at sufficiently high energy.

## 6 Acknowledgments

We would like to thank W.G. Lynch, M.B. Tsang and V. Zelevinsky for discussions of various parts of this work. FTD and MD acknowledge the support of FAPESP. TJS acknowledges the support of CAPES. RD and SRS acknowledge partial support from the CNPq. BVC acknowledges partial support from CAPES, the CNPq and FAPESP.

## A Appendix

The extended Hauser-Feshbach model takes energy and angular momentum conservation into account in its description of particle and fragment evaporation. The model is formulated in terms of quantized

angular momenta and is thus conceptually sound. However, the sums over angular momenta in its expressions for decay widths, especially in the case of intermediate fragment emission, can be cumbersome and computationally expensive. Here, we develop an alternative model in terms of classical angular momenta, formulated long ago by Ericson and Strutintsky [18, 19], which permits simpler estimates of the decay widths.

### A.1 Classical phase space volumes

The position and orientation of a rigid body can be expressed in terms of the three coordinates of its center-of-mass, $\vec{r}$, and the three Euler angles, $\phi$, $\theta$, $\psi$, that define a rotation from a fixed orientation. The variables conjugate to these can be taken as the three components of the linear momentum, $\vec{p}$, and of the angular momentum, $\vec{J}$. We can thus write the phase space volume element of a rigid body as

$$\frac{1}{(2\pi\hbar)^6} d^3r\, d^3p\, d\phi\, d\cos\theta\, d\psi\, d^3J\,. \tag{A.1}$$

For the moment, we neglect the effects of orientation of the rigid body and simply integrate it out ($d\phi\, d\cos\theta\, d\psi \rightarrow 2\pi \cdot 2 \cdot 2\pi = 8\pi^2$). We want to include the remaining terms, $8\pi^2 d^3J/(2\pi\hbar)^3 = d^3J/\left(\pi\hbar^3\right)$, in an extended phase space integral. We show that such a procedure is not unreasonable, by demonstrating that it furnishes expressions similar to the quantum mechanical ones. We begin with the usual Bethe ansatz to the spin distribution - we assume that the density of states with energy $\varepsilon$ and spin projection quantum number $m$ can be approximated as

$$\omega(\varepsilon, m) = \omega(\varepsilon)\, \frac{1}{\sqrt{2\pi\sigma^2}} \exp\left[-m^2/2\sigma^2\right], \tag{A.2}$$

where $\sigma$ is an energy-dependent spin cutoff factor. We can then determine the density of levels of total spin quantum number $j$ as

$$\tilde{\rho}(\varepsilon,\ j) = \omega(\varepsilon,\ m = j) - \omega(\varepsilon,\ m = j+1) \approx (2j+1)\, \omega(\varepsilon)\, \frac{\exp\left[-(j+1/2)^2/2\sigma^2\right]}{\sqrt{\pi}\,(2\sigma^2)^{3/2}}\,. \tag{A.3}$$

We find for the total density of states

$$\omega(\varepsilon) = \sum_{j=0}^{j_{max}} (2j+1)\, \tilde{\rho}(\varepsilon,\ j) \approx \sum_{j=0}^{j_{max}} (2j+1)^2\, \omega(\varepsilon)\, \frac{\exp\left[-j(j+1)/2\sigma^2\right]}{\sqrt{\pi}\,(2\sigma^2)^{3/2}}\,, \tag{A.4}$$

which implies that the total density of levels is

$$\tilde{\rho}(\varepsilon) = \sum_{j=0}^{j_{max}} \tilde{\rho}(\varepsilon,\ j) \approx \frac{1}{\sqrt{2\pi\sigma^2}}\omega(\varepsilon)\,. \tag{A.5}$$

If we consider a classical density of the form,

$$\rho\left(\varepsilon,\ \vec{J}\right) = \omega(\varepsilon)\, \frac{\exp\left[-\vec{J}^2/\left(2\sigma^2\hbar^2\right)\right]}{\left(2\pi\sigma^2\hbar^2\right)^{3/2}}\,, \tag{A.6}$$

we obtain a similar result when we calculate

$$\begin{aligned}\omega(\varepsilon) &= \int \rho\left(\varepsilon, \vec{J}\right) d^3J \\ &= \frac{1}{\hbar^3}\int (2J)^2\omega(\varepsilon)\,\frac{\exp\left[-\vec{J}^2/\left(2\sigma^2\hbar^2\right)\right]}{\sqrt{\pi}\,(2\sigma^2)^{3/2}}dJ \\ &= \int (2j)^2\omega(\varepsilon)\,\frac{\exp\left[-j^2/2\sigma^2\right]}{\sqrt{\pi}\,(2\sigma^2)^{3/2}}dj\end{aligned} \tag{A.7}$$

and associate the spin quantum number $j$ to the magnitude of the spin $J$ through $J = j\hbar$. We note that, technically, the level density is $(2j+1)$ times the quantity given in Eq. (A.6), but for convenience we will continue to use the term to describe the density of that equation.

For a particle with spin multiplicity $g$ but no excited states, we take

$$\rho\left(\varepsilon, \vec{J}\right) = \frac{1}{\pi\hbar^2 g}\delta(J - g\hbar/2)\,\delta(\varepsilon)\,, \tag{A.8}$$

where $g = 2s+1$ is the spin multiplicity, so that

$$\int \rho\left(\varepsilon, \vec{J}\right) d^3J = g\delta(\varepsilon) = \omega(\varepsilon)\,. \tag{A.9}$$

We next decompose the momentum into its radial and angular components,

$$p_r = \vec{p}\cdot\hat{r} \qquad \text{and} \qquad \vec{p}_\theta = \vec{p} - p_r\hat{r}\,, \tag{A.10}$$

and rewrite the latter in terms of the orbital angular momenta,

$$\vec{r}\times\vec{p} = r\times\vec{p}_\theta = \vec{L}\,. \tag{A.11}$$

Since the angular components of the momenta as well as the two components of the corresponding angular momenta are perpendicular to the coordinate vector, we can rewrite the differential as

$$d^3p\,d^3r = dp_r\,d^2p_\theta\,r^2dr\,d\Omega = dp_r\,d^2L\,dr\,d\Omega\,. \tag{A.12}$$

Like its conjugate solid angle $\Omega$, the orbital angular momentum is a two-dimensional quantity rather than a three-dimensional one. We can extend the latter to a three-dimensional quantity and make its orthogonality to the radial motion explicit by introducing a $\delta$-function into the phase space differential,

$$dp_r\,d^2L\,dr\,d\Omega = \delta\left(\hat{r}\cdot\vec{L}\right)dp_r\,d^3L\,dr\,d\Omega\,, \tag{A.13}$$

as was done by Ericson and Strutintsky in their semiclassical description of compound nucleus decay.

### A.2 Decay rates and partial widths

We now consider the decay of a compound nucleus of charge $Z_0$, mass number $A_0$, excitation energy $\varepsilon_0$ and (classical) angular momentum $\vec{J}_0$ into fragments 1 and 2 of charge $Z_1$ and $Z_2$ and mass number $A_1$ and $A_2$. The rate at which this decay occurs is proportional to the rate at which the compound nucleus separates into the two fragments, which in turn is proportional to

$$\frac{p_r}{\mu}\theta(p_r)\,\delta(r - R_B)\,\rho_1\left(\varepsilon_1, \vec{J}_1\right)\rho_2\left(\varepsilon_2, \vec{J}_2\right)\,, \tag{A.14}$$

where the first factor is the positive relative velocity with which the two fragments pass the radius $R_B$ and the last two terms are the densities of levels of the emitted fragments, $\varepsilon_1$ and $\varepsilon_2$ being their excitation energies and $\vec{J}_1$ and $\vec{J}_2$ their angular momenta. It is reasonable to choose the value of the separation radius $R_B$ as the value at which the barrier between the two fragments is at is maximum, as beyond this radius there is, in principle, no impediment to their separation. We obtain the partial width for this process, $\Gamma(\varepsilon_0,\, \vec{J}_0; Z_1A_1,\, Z_2A_2)$, by summing over all possible configurations, taking into account conservation of energy and angular momentum and inserting the appropriate phase space factors. We have

$$\begin{aligned} 2\pi\Gamma(\varepsilon_0,\, \vec{J}_0; Z_1A_1,\, Z_2A_2)\rho_0\left(\varepsilon_0,\, \vec{J}_0\right) &= \frac{1}{(2\pi\hbar)^2}\int \frac{p_r}{\mu}\theta\left(p_r\right)\delta\left(r - R_B\right)\delta\left(\hat{r}\cdot\vec{L}\right) dp_r\, d^3L\, dr\, d\Omega \\ &\times \prod_{j=1}^{2}\left(\rho_j\left(\varepsilon_j,\, \vec{J}_j\right) d\varepsilon_j d^3J_j\right)\delta\left(\vec{J}_0 - \vec{L} - \vec{J}_1 - \vec{J}_2\right) \quad \text{(A.15)} \\ &\times \delta\left(\varepsilon_0 - B_0 - \frac{p_r^2}{2\mu} - \frac{L^2}{2\mu R_B^2} - V_B - \sum_{j=1}^{2}\left(\varepsilon_j - B_j\right)\right), \end{aligned}$$

where $\rho_0\left(\varepsilon_0,\, \vec{J}_0\right)$ is the level density of the compound nucleus, $B_0$, $B_1$ and $B_2$ are the binding energies of the compound nucleus and the two fragments and $V_B$ is the barrier height at the radius $R_B$. We combine these into the $Q$ of the reaction as

$$Q = B_0 - B_1 - B_2 \tag{A.16}$$

and note that the radial momentum terms can be rewritten in terms of the radial energy, $e_r$,

$$\frac{p_r}{\mu}\theta\left(p_r\right) dp_r \rightarrow \frac{1}{2} de_r\,. \tag{A.17}$$

After performing the integral over the radial coordinate, we can rewrite the expression for the partial width as

$$\begin{aligned} 2\pi\Gamma(\varepsilon_0,\, \vec{J}_0; Z_1A_1,\, Z_2A_2)\rho_0\left(\varepsilon_0,\, \vec{J}_0\right) &= \frac{1}{2\,(2\pi\hbar)^2}\int \delta\left(\hat{r}\cdot\vec{L}\right) d^3L\, d\Omega\, de_r \quad \text{(A.18)} \\ &\times \prod_{j=1}^{2}\left(\rho_j\left(\varepsilon_j,\, \vec{J}_j\right) d\varepsilon_j d^3J_j\right)\delta\left(\vec{J}_0 - \vec{L} - \vec{J}_1 - \vec{J}_2\right) \\ &\times \delta\left(\varepsilon_0 - Q - e_r - \frac{L^2}{2\mu R_B^2} - V_B - \varepsilon_1 - \varepsilon_2\right). \end{aligned}$$

When one of the fragments is a particle (for which we neglect any excited states), we neglect its contribution to angular momentum conservation and perform the integrals over its excitation energy and angular momentum (see Eqs. (A.8) and (A.9)) to obtain

$$\begin{aligned} 2\pi\Gamma(\varepsilon_0,\, \vec{J}_0; Z_1A_1,\, Z_2A_2)\rho_0\left(\varepsilon_0,\, \vec{J}_0\right) &= \frac{1}{2\,(2\pi\hbar)^2} g\int \delta\left(\hat{r}\cdot\vec{L}\right) d^3L\, d\Omega\, de_r \quad \text{(A.19)} \\ &\times \rho_2\left(\varepsilon_2,\, \vec{J}_2\right) d\varepsilon_2 d^3J_2\,\delta\left(\vec{J}_0 - \vec{L} - \vec{J}_2\right) \\ &\times \delta\left(\varepsilon_0 - Q - e_r - \frac{L^2}{2\mu R_B^2} - V_B - \varepsilon_2\right). \end{aligned}$$

If we rewrite this in terms of the asymptotic kinetic energy

$$e = e_r + \frac{L^2}{2\mu R_B^2} + V_B \tag{A.20}$$

and perform the angular integral, we have

$$\begin{aligned} 2\pi\Gamma(\varepsilon_0,\, \vec{J_0}; Z_1A_1,\, Z_2A_2)\rho_0\left(\varepsilon_0,\, \vec{J_0}\right) &= \frac{1}{4\pi\hbar^2} g \int L\, dL\, d\Omega_L\, de\, \theta\left(e - \frac{L^2}{2\mu R_B^2} - V_B\right) \\ &\quad \times \rho_2\left(\varepsilon_2,\, \vec{J_2}\right) d\varepsilon_2 d^3J_2\, \delta\left(\vec{J_0} - \vec{L} - \vec{J_2}\right) \\ &\quad \times \delta\left(\varepsilon_0 - Q - e - \varepsilon_2\right) . \end{aligned} \tag{A.21}$$

If we now rewrite the Heaviside step function as a transmission coefficient,

$$\theta\left(e - \frac{L^2}{2\mu R_B^2} - V_B\right) \to T_L\left(e\right) \approx \left(1 + \exp\left[\left(e - \frac{L^2}{2\mu R_B^2} - V_B\right)/\hbar\omega\right]\right)^{-1} , \tag{A.22}$$

we obtain the expression given by Ericson and Strutinsky,

$$\begin{aligned} 2\pi\Gamma(\varepsilon_0,\, \vec{J_0}; Z_1A_1,\, Z_2A_2)\rho_0\left(\varepsilon_0,\, \vec{J_0}\right) &= \frac{1}{4\pi\hbar^2} g \int L\, dL\, d\Omega_L\, de\, T_L\left(e\right) \\ &\quad \times \rho_2\left(\varepsilon_2,\, \vec{J_2}\right) d\varepsilon_2 d^3J_2\, \delta\left(\vec{J_0} - \vec{L} - \vec{J_2}\right) \\ &\quad \times \delta\left(\varepsilon_0 - Q - e - \varepsilon_2\right) , \end{aligned} \tag{A.23}$$

up to a factor of 1/2.

If we make the assumption that the $\vec{J_2}$ dependence of the level density $\rho_2\left(\varepsilon_2,\, \vec{J_2}\right)$ is so small in the relevant range of values that it can be neglected, (which only makes sense if the same approximation applies to $\vec{J_0}$),we can take

$$\rho_2\left(\varepsilon_2,\, \vec{J_2}\right) \to \rho_2\left(\varepsilon_2,\, 0\right) \qquad \text{and} \qquad \rho_0\left(\varepsilon_0,\, \vec{J_0}\right) \to \rho_0\left(\varepsilon_0,\, 0\right) \tag{A.24}$$

and evaluate the integrals over $\Omega_L$, $\vec{J_2}$ and $\varepsilon_2$ to obtain

$$2\pi\Gamma(\varepsilon_0,\, \vec{J_0}; Z_1A_1,\, Z_2A_2)\rho_0\left(\varepsilon_0,\, 0\right) = \frac{1}{\hbar^2} g \int L\, dL\, T_L\left(e\right)\, \rho_2\left(\varepsilon_0 - Q - e,\, 0\right)\, de\, . \tag{A.25}$$

The integral over $L$ furnishes

$$\frac{1}{\hbar^2} \int L\, dL\, T_L\left(e\right) = \frac{\mu e}{\pi\hbar^2} \sigma_{inv}\left(e\right) , \tag{A.26}$$

where $\sigma_{inv}\left(e\right)$ is the cross section for formation of the compound nucleus from the residual nucleus and the emitted particle. Substituting in the preceding expression, we obtain the Weisskopf approximation to the partial width,

$$2\pi\Gamma(\varepsilon_0,\, \vec{J_0}; Z_1A_1,\, Z_2A_2)\rho_0\left(\varepsilon_0,\, 0\right) = \frac{g\mu}{\pi\hbar^2} \int e\, \sigma_{inv}\left(e\right)\, \rho_2\left(\varepsilon_0 - Q - e,\, 0\right)\, de\, , \tag{A.27}$$

again up to a factor of 1/2. As this factor enters all the partial widths, it cancels out when the branching ratios are considered.

### A.3 Approximate width for intermediate mass fragment emission

In his section, we wish to obtain an approximate expression for the intermediate mass fragment emission width of Eq. (A.18), which we repeat here,

$$\begin{aligned} 2\pi\Gamma(\varepsilon_0,\,\vec{J_0};Z_1A_1,\,Z_2A_2)\rho_0\left(\varepsilon_0,\,\vec{J_0}\right) &= \frac{1}{2\,(2\pi\hbar)^2}\int \delta\left(\hat{r}\cdot\vec{L}\right)\,d^3L\,d\Omega\,de_r \\ &\times\prod_{j=1}^{2}\left(\rho_j\left(\varepsilon_j,\,\vec{J_j}\right)d\varepsilon_j d^3J_j\right)\delta\left(\vec{J_0}-\vec{L}-\vec{J_1}-\vec{J_2}\right) \\ &\times\delta\left(\varepsilon_0-Q-e_r-\frac{L^2}{2\mu R_B^2}-V_B-\varepsilon_1-\varepsilon_2\right). \end{aligned}$$

To evaluate this expression, we use an approximate Fermi gas form of the level densities, taking

$$\omega_j\left(\epsilon_j\right)=\frac{\sqrt{\pi}}{12}\frac{cA_j}{\left(\sqrt{cA_j\epsilon_j}+2\right)^{5/2}}\exp\left[2\sqrt{cA_j\epsilon_j}\right], \tag{A.28}$$

and

$$\rho_j\left(\varepsilon_j,\,\vec{J_j}\right)=\frac{1}{\left(2\pi I_jT_j\right)^{3/2}}\omega_j\left(\epsilon_j\right), \tag{A.29}$$

where we take $\epsilon_j$ to be the thermal excitation energy, given by the difference between the total excitation energy and its collective rotational component,

$$\epsilon_j=\varepsilon_j-\frac{J^2}{2I_j}, \tag{A.30}$$

with $I_j$ the moment of inertia, $cA_j$ is the level density parameter, with $c\approx 1/7$-$1/8$ Mev$^{-1}$and $T_j$ the effective temperature, given by

$$\frac{1}{T_j}=\frac{1}{\rho_j\left(\varepsilon_j,\,\vec{J_j}\right)}\frac{\partial\rho_j\left(\varepsilon_j,\,\vec{J_j}\right)}{\partial\varepsilon_j}=\frac{cA_j}{\sqrt{cA_j\epsilon_j}+2}. \tag{A.31}$$

The factor $cA_j/\left(\sqrt{cA_j\epsilon_j}+2\right)^{5/2}$ is used here in place of the expected factor $cA_j/\left(cA_j\epsilon_j\right)^{5/4}$ to guarantee the correct behavior of the density at low and high excitation energies.

We approximate this integral by expanding around its maximum, given by the condition of thermal equilibrium, which we approximate as ,

$$\epsilon_{10}=\frac{A_1}{A_0}\epsilon_0, \qquad \epsilon_{20}=\frac{A_2}{A_0}\epsilon_0, \tag{A.32}$$

corresponding to a common temperature of

$$T_0=\sqrt{\frac{\epsilon_0}{cA_0}}+\frac{2}{cA_0}. \tag{A.33}$$

as well as the sticking condition,

$$\vec{L}_0=\frac{\mu R_B^2}{I_T}\vec{J}_0, \qquad \vec{J}_{10}=\frac{I_1}{I_T}\vec{J}_0, \qquad \vec{J}_{20}=\frac{I_2}{I_T}\vec{J}_0, \tag{A.34}$$

where $I_T$ is the total moment of inertia at the barrier (scission point),

$$I_T = \mu R_B^2 + I_1 + I_2 \,, \tag{A.35}$$

and

$$\epsilon_0 = \epsilon_{10} + \epsilon_{20} = \varepsilon_0 - Q - V_B - \frac{J_0^2}{2I_T} \,. \tag{A.36}$$

These conditions are consistent with a picture at scission of two fragments in thermal equilibrium that are rotating with a scission point fixed in the rotating frame.

We approximate the radial angular integral as

$$\int \delta\left(\hat{r}\cdot\vec{L}\right) d\Omega = 2\pi\frac{1}{L} \to 2\pi\frac{1}{L_0} \to 2\pi\frac{I_T}{\mu R_B^2}\frac{2}{2J_0+\hbar} \,. \tag{A.37}$$

The angular momentum integrals then yield

$$\begin{aligned}
&\frac{1}{(2\pi T_0)^3\,(I_1 I_2)^{3/2}} \int \exp\left[-\frac{L^2}{2T_0\mu R_B^2} - \frac{J_1^2}{2T_0 I_1} - \frac{J_2^2}{2T_0 I_2}\right] \delta\left(\vec{J}_0 - \vec{L} - \vec{J}_1 - \vec{J}_2\right) d^3L\, d^3J_1\, d^3J_2 \\
&\quad\to \frac{1}{(2\pi T_0)^3\,(I_1 I_2)^{3/2}} \int \exp\left[-\frac{\left(\begin{array}{cc}\delta\vec{L}, & \delta\vec{J}_1\end{array}\right)}{2T_0} \left(\begin{array}{cc} \frac{1}{\mu R_B^2}+\frac{1}{I_2} & \frac{1}{I_2} \\ \frac{1}{I_2} & \frac{1}{I_1}+\frac{1}{I_2}\end{array}\right) \left(\begin{array}{c}\delta\vec{L}\\ \delta\vec{J}_1\end{array}\right)\right] d^3\delta L\, d^3\delta J_1 \\
&\qquad = \frac{1}{(I_1 I_2)^{3/2}} \det\left|\begin{array}{cc} \frac{1}{\mu R_B^2}+\frac{1}{I_2} & \frac{1}{I_2} \\ \frac{1}{I_2} & \frac{1}{I_1}+\frac{1}{I_2}\end{array}\right|^{-3/2} = \left(\frac{\mu R_B^2}{I_T}\right)^{3/2} ,
\end{aligned} \tag{A.38}$$

where $\delta\vec{L} = \vec{L} - \vec{L}_0$ and $\delta\vec{J}_1 = \vec{J}_1 - \vec{J}_{10}$, so that

$$\begin{aligned}
2\pi\Gamma(\varepsilon_0,\, \vec{J}_0; Z_1A_1,\, Z_2A_2)\rho_0\left(\varepsilon_0,\, \vec{J}_0\right) &= \frac{1}{2\pi\hbar^2}\left(\frac{\mu R_B^2}{I_T}\right)^{1/2} \frac{1}{2J_0+\hbar} \\
&\quad\times \int \omega_1\left(\epsilon_1\right)\omega_2\left(\epsilon_0-\epsilon_1-e_r\right)\, d\epsilon_1\, de_r \,.
\end{aligned} \tag{A.39}$$

The excitation energy integral about the maximum value of the integrand furnishes

$$\begin{aligned}
\int \omega_1\left(\epsilon_1\right)\omega_2\left(\epsilon_0-\epsilon_1-e_r\right)\, d\epsilon_1 &\to \omega_1\left(\epsilon_{10}-\frac{A_1}{A_0}e_r\right)\omega_2\left(\epsilon_{20}-\frac{A_2}{A_0}e_r\right) \\
&\quad\times \int \exp\left[\left(\frac{dT_1^{-1}}{d\epsilon_1}+\frac{dT_2^{-1}}{d\epsilon_2}\right)\frac{\left(\epsilon_1-\epsilon_{10}+\frac{A_1}{A_0}e_r\right)^2}{2}\right] d\epsilon_1 \\
&\approx \left(4\pi\frac{A_1A_2}{A_0}cT_0^3\right)^{1/2} \omega_1\left(\epsilon_{10}-\frac{A_1}{A_0}e_r\right)\omega_2\left(\epsilon_{20}-\frac{A_2}{A_0}e_r\right) ,
\end{aligned} \tag{A.40}$$

in the high-energy limit, in which $T_j \to \sqrt{\epsilon_j/cA_j}$, so that

$$\begin{aligned}
2\pi\Gamma(\varepsilon_0,\, \vec{J}_0; Z_1A_1,\, Z_2A_2)\rho_0\left(\varepsilon_0,\, \vec{J}_0\right) &= \frac{1}{2\pi\hbar^2}\left(\frac{\mu R_B^2}{I_T}\right)^{1/2} \frac{1}{2J_0+\hbar}\left(4\pi\frac{A_1A_2}{A_0}cT_0^3\right)^{1/2} \\
&\quad\times \int \omega_1\left(\epsilon_{10}-\frac{A_1}{A_0}e_r\right)\omega_2\left(\epsilon_{20}-\frac{A_2}{A_0}e_r\right) de_r \,,
\end{aligned} \tag{A.41}$$

Finally, we approximate the integral over the relative escape energy as

$$2\pi\Gamma(\varepsilon_0,\,\vec{J_0};Z_1A_1,\,Z_2A_2)\rho_0\left(\varepsilon_0,\,\vec{J_0}\right) = \frac{1}{2\pi\hbar^2}\left(4\pi\frac{A_1A_2}{A_0}\frac{\mu R_B^2}{I_T}cT_0\right)^{1/2}\frac{T_0}{2J_0+\hbar} \times\omega_1\left(\epsilon_{10}\right)\omega_2\left(\epsilon_{20}\right)\int\exp\left(-e_r/T_0\right)de_r\,, \tag{A.42}$$

$$= \frac{1}{2\pi\hbar^2}\left(4\pi\frac{A_1A_2}{A_0}\frac{\mu R_B^2}{I_T}cT_0\right)^{1/2}\frac{T_0^2}{2J_0+\hbar}\omega_1\left(\epsilon_{10}\right)\omega_2\left(\epsilon_{20}\right)\,.$$

We used an extended version of this expression containing a transmission factor some time ago, to study the effects of the formation of a dinuclear system onlight-ion fusion.[33] The code GEMINI++ calculates this integral numerically. It does so by expressing the product of densities in terms of the density of scission states,

$$\rho_{sc}\left(\epsilon_0-e_r,\,\vec{J_0}\right) = \frac{1}{(2\pi I_T T_0)^{3/2}}\omega_0\left(\epsilon_0-e_r\right). \tag{A.43}$$

We approximate this using the high-energy limit of the densities, which furnishes

$$\omega_1\left(\epsilon_{10}-\frac{A_1}{A_0}e_r\right)\omega_2\left(\epsilon_{20}-\frac{A_2}{A_0}e_r\right)\approx\left(\frac{A_0^2}{A_1A_2}\frac{1}{cA_0}\right)^{3/2}\frac{1}{T_0^{5/2}}\,\omega_0\left(\epsilon_0-e_r\right)\,, \tag{A.44}$$

so that

$$2\pi\Gamma(\varepsilon_0,\,\vec{J_0};Z_1A_1,\,Z_2A_2)\rho_0\left(\varepsilon_0,\,\vec{J_0}\right) = \frac{2\pi}{2j_0+1}\left(2\frac{\mu R_B^2}{I_T}cA_0T_0\right)^{1/2}\frac{A_0^2}{A_1A_2} \times\left(\frac{I_T}{\hbar^2cA_0}\right)^{3/2}\int\rho_{sc}\left(\epsilon_0-e_r,\,\vec{J_0}\right)de_r\,, \tag{A.45}$$

where $j_0 = J_0/\hbar$ is the quantum number corresponding to the value of the total angular momentum. The integral can be well approximated similarly to that in Eq. (A.42), yielding

$$2\pi\Gamma(\varepsilon_0,\,\vec{J_0};Z_1A_1,\,Z_2A_2)\rho_0\left(\varepsilon_0,\,\vec{J_0}\right) = \frac{2\pi}{2j_0+1}\left(2\frac{\mu R_B^2}{I_T}cA_0T_0\right)^{1/2}\frac{A_0^2}{A_1A_2} \times T_0\left(\frac{I_T}{\hbar^2cA_0}\right)^{3/2}\rho_{sc}\left(\epsilon_0,\,\vec{J_0}\right)\,. \tag{A.46}$$

## References


[1] N. Bohr, Nature **137** (1936) 344.
[2] H. A. Bethe, Rev. Mod. Phys. **9** (1937) 69.
[3] C. Bloch, Phys. Rev. **93** (1954) 1094.
[4] C. Bloch, Statistical Nuclear Theory, Les Houches Lectures (1968) 305.
[5] A. Bohr and B.R. Mottelson, in Nuclear Structure, vol. 1 (Benjamin, Reading, Mass., 1969) p.281
[6] M. Brack and Ph. Quentin, Phys. Lett. **52B**, 159 (1974).
[7] M. Brack and Ph. Quentin, Physica Scripta **A10**, 163 (1974).

[8] P. Bonche, S. Levit and D. Vautherin, Nucl. Phys. **A427**, 278 (1984).
[9] P. Bonche, S. Levit and D. Vautherin, Nucl. Phys. **A436**, 265 (1985).
[10] G. A. Lalazissis, J. König and P. Ring, Phys.Rev. C **55**, 540 (1997).
[11] T. Niksic, D. Vretenar, P. Finelli, and P.Ring, Phys. Rev. C **66**, 024306 (2002).
[12] S. Goriely, M. Samyn, and J. Pearson, Phys. Rev. C **75**, 064312 (2007).
[13] A. W. Steiner, M. Prakash, J. M. Lattimer, and P. J. Ellis, Phys. Rep., 325 **411** (2005).
[14] R. Lisboa, M. Malheiro, and B. V. Carlson, IJMP **16**, 3032 (2007).
[15] V.F. Weisskopf, Phys. Rev. **52**, 295 (1937).
[16] V.F. Weisskopf and D.H. Ewing, Phys. Rev. 57 (1940) 472, 935.
[17] W. Hauser and H. Feshbach, Phys Rev. 87 (1952) 366.
[18] T. Ericson and V. Strutintsky, Nucl. Phys. **8**, 284 (1958); **9**, 689 (1958).
[19] T. Ericson, Adv. Phys. **9**, 425 (1960).
[20] J. P. Bondorf, R. Donangelo, I. N. Mishustin, C. J. Pethick, H. Schulz and, K. Sneppen, Nucl Phys. **A443**, 321 (1985); Nucl. Phys. **A444**, 460 (1985); Nucl. Phys. **A448**, 753 (1986).
[21] A. S. Botvina, A. S. Iljinov, I. N. Mishustin, J. P. Bondorf, R. Donangelo, K. Sneppen, Nucl. Phys. **A475**, 663 (1987); J. P. Bondorf, A. S. Botvina, A. S. Iljinov, I. N. Mishustin, K. Sneppen, Phys. Rep. **257**, 133 (1995).
[22] E. Fermi, Prog. Theor. Phys. **5**, 570 (1950).
[23] B.V. Carlson, R. Donangelo, S.R. Souza, W.G. Lynch, A.W. Steiner, M.B. Tsang, Nucl. Phys. **A876**, 77 (2012).
[24] W. A. Friedman and W. G. Lynch, Phys. Rev. C **28**, **16** (1983).
[25] B.V. Carlson, F.T. Dalmolin, M. Dutra, R. Donangelo, S.R. Souza, D.A. Toneli, Proceedings of the 13th International Conference on Nuclear Reaction Mechanisms, CERN Proceedings 2012, 285 (2012).
[26] R. J. Charity, in Proceedings of the Joint ICTP-IAEA Advanced Workshop on Model Codes for Spallation Reactions (IAEA, Triste, Italy, 2008); edited by D. Filges, S. Leray, Y. Yariv, A. Mengoni, A. Stanculescu and G. Mank, INDC(NDS)-530, 139 (2008).
[27] R. J. Charity, Phys. Rev. C **82**, 014610 (2010).
[28] D. Mancusi, R. J. Charity, J. Cugnon,Phys. Rev. C **82**, 044610 (2010).
[29] N. Frazier, B.A. Brown, V. Zelevinsky, Phys. Rev. C **54**, 165 (1996).
[30] D. Mancusi, J. Cugnon, A. Boudard, J.-C. David, S. Leray, R. J. Charity, A. Kelic-Heil, M. V. Ricciardi, Journal of the Korean Physical Society **59**, 943 (2011).
[31] W. Gawlikowicz, Acta. Phys. Pol. B **28**, 1687 (1997).
[32] J.B. Natowitz, R. Wada, K. Hagel, T. Keutgen, M. Murray, A. Makeev, L. Qin, P. Smith, C. Hamilton, Phys. Rev. C **65**, 034618 (2002).
[33] B. V. Carlson, O. Civitarese, M. S. Hussein, A. Szanto de Toledo, Ann. Phys. (N.Y.) **169**, 167 (1986).